Characterization of chemical-vapor-deposited low-*k* thin films using x-ray porosimetry

Hae-Jeong Lee,[a] Eric K. Lin, Barry J. Bauer, and Wen-li Wu
Polymers Division, National Institute of Standards and Technology, Gaithersburg, Maryland 20899

Byung Keun Hwang and William D. Gray
Advanced Materials Business Electronic Industry, Dow Corning, 22 West Salzburg Road, Midland, Michigan 48686

(Received 27 August 2002; accepted 20 December 2002)

Trimethylsilane-based carbon-doped silica films prepared with varying chemical-vapor-deposition process conditions were characterized using x-ray reflectivity and porosimetry to measure the film thickness, average film density, density depth profile, wall density, and porosity. Samples deposited under single or dual frequency conditions with either N_2O or O_2 as an oxidant were compared. The structural parameters were correlated with the chemical bond structure measured by Fourier transform infrared spectroscopy. The density profiles of the porous films were uniform with a slight densification at the film surface. The distribution of pores was also uniform through the film. Films prepared under a single frequency and/or N_2O atmosphere had the lowest film density, wall density, and dielectric constant. The porosities of the films were similar and the pore sizes were less than 10 Å. © *2003 American Institute of Physics.* [DOI: 10.1063/1.1553996]

In next generation devices with dimensions below 0.13 μm, increases in propagation delay, cross talk noise, and power dissipation of the interconnect structure become limiting factors for integrated circuits (ICs). To address these problems, new low dielectric constant (low-*k*) interlayer dielectric materials are being developed to replace silica.[1] Low-*k* CVD films have attracted interest due to their physical rigidity, superior mechanical strength, and compatibility with current Si technology. Recently, an ultralow-*k* CVD film with voids has been prepared showing the potential of porous CVD films in future interconnect structures.[2]

In porous low-*k* materials, the pore structure seriously affects other crucial properties. It is essential to have methods to characterize the on-wafer structure of these porous thin films to optimize processing conditions and the resulting physical properties.[3,4] We have previously reported the results of porous thin films prepared by a spin-on technique using a combination of specular x-ray reflectivity (SXR), small angle neutron scattering (SANS), and an ion scattering technique.[5] Although this combination of techniques is promising for the characterization of the structural properties of porous thin films with pores larger than 10 Å, SANS measurements are not sensitive to micropores with sizes below 10 Å because the probing wavelength is 6 Å.

In this work, we demonstrate the use of x-ray porosimetry (XRP) as a method to obtain structural information about CVD low-*k* thin films with small pore sizes and low porosity using an SXR technique. One of the candidates for CVD low-*k* thin films is trimethylsilane (3 MS)-based carbon-doped silica film (α-SiCO:H). Low-*k* α-SiCO:H thin films with dielectric constants ranging from 2.6 to 2.9 were prepared using single or dual frequency modes with different oxidants, O_2 or N_2O from Dow Corning® Z3MS (Ref. 6). Details about the process conditions are described elsewhere.[7] The elemental compositions of the films were determined using Rutherford backscattering spectrometry and forward recoil spectrometry.

SXR measurements were performed using a modified high-resolution x-ray diffractometer. The wavelength, λ, was 1.54 Å. The reflected intensity was collected as a function of the incident angle. SXR data were used to measure the thickness, average mass density, and density depth profile of the thin films. XRP was employed to characterize the porosity and wall density of the thin films. Measurements were performed on samples in a vacuum and under a saturated toluene atmosphere, where liquid toluene condensed in interconnected pores. Evacuated samples were measured in a conventional manner reported elsewhere after evacuation for 2 h.[8] The saturated environment is created by placing a container of liquid toluene inside the SXR chamber. The samples were saturated under a toluene atmosphere for 2 h before measuring the x-ray reflectivity. The results from XRP were compared with those from SANS data. SANS measurements were performed with a neutron wavelength of 6 Å with a wavelength spread, $\Delta\lambda/\lambda$, of 0.14. Scattering measurements were conducted under a vacuum to determine the average pore size of the pores in the films. The influence of the process conditions on the chemical bonding structures was investigated using Fourier transform infrared (FTIR) spectroscopy with $4 \pm 0.01\ \mathrm{cm}^{-1}$ spectral resolution. The dielectric constant was measured on silicon–insulator–metal structures using highly doped silicon substrates and Al dot structures.

Figure 1 shows SXR experimental data and the best fit to the data from CVD films after varying process conditions. The SXR profile of the film is plotted as the logarithm of the reflected intensity (I_r/I_0) as a function of momentum transfer, q ($q=(4\pi/\lambda)\sin\theta$), where, θ is the grazing incident angle of the x-ray beam. The reflectivity drops sharply as the x-ray beam begins to penetrate the film after a critical value,

[a]Author to whom correspondence should be addressed; electronic mail: haejeong.lee@nist.gov

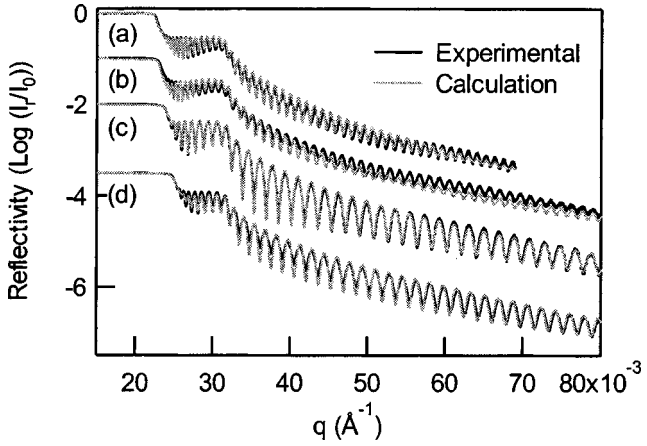

FIG. 1. SXR curves and the best fit to the data of α-SiCO:H films prepared under different process conditions, (a) N_2O and single frequency, (b) N_2O and dual frequency, (c) O_2 and single frequency, and (d) O_2 and dual frequency. The black and gray curves represent the experimental and calculated data, respectively. The curves are offset for clarity.

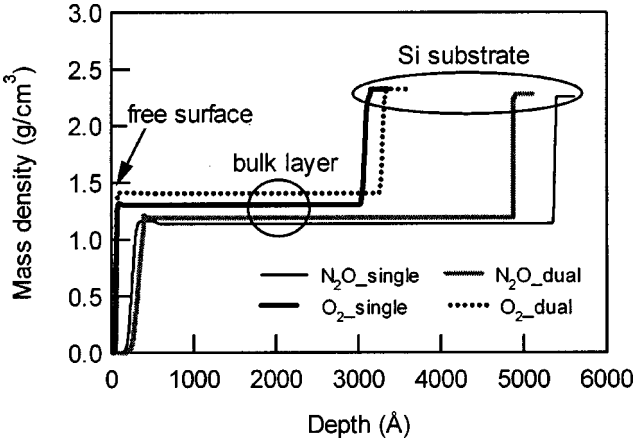

FIG. 2. Calculated electron density depth profile of α-SiCO:H films in Fig. 1. The free surface is located at the far left-hand side of the horizontal axis and the silicon substrate is located at the far right-hand side of the abscissa.

q_c. The critical angle, in units of $q_c^2(\text{Å}^{-2})$, is used to calculate the average mass density of the film. The measured critical angles show that the highest density film was prepared under dual frequency using O_2 gas as an oxidant and the lowest density film was prepared under single frequency using N_2O gas as an oxidant. These results are consistent with the dielectric constant of each film. The average mass densities ranged from 1.17 g/cm^3 to 1.43 g/cm^3, which are significantly lower than the density of films prepared from PECVD, 2.27 g/cm^3.[9] The dielectric constant, elemental composition, and average film density are summarized in Table I.

The SXR data were fit by comparing model electron density profiles to the experimental data using a least-squares fitting routine based on the algorithm of Parrat.[10] Film thicknesses determined from fitting of x-ray reflectivity curves are listed in Table I. In Fig. 2, the corresponding electron density depth profiles for the SXR data of Fig. 1 show very uniform electron density profiles with a thin denser layer at the free surface of the films. The thickness of the denser layer ranged from (60 ± 10) Å to (300 ± 10) Å and the increases in electron density of this layer are approximately 0.4% higher than that of the bulk layer.[11] A native oxide layer approximately 50 Å thick was also detected between the low-k film and the silicon surface. The measurement of these subtle density differences illustrates the sensitivity and resolution of the SXR technique.

The sensitivity and resolution of SXR are sufficient to distinguish the average density of films between under a vacuum and in the saturated toluene. In Fig. 3, the critical angle of the porous film increases in the presence of toluene vapor. This is due to capillary condensation of the toluene inside pores accessible to the solvent vapor. The condensation of toluene into these pores decreases the effective porosity and appears as an increase in the average density of the film. The average mass density of the film is related to the porosity and matrix density of the film through the rule of mixtures in $\rho_{\text{ave}}=\rho_w\times(1-P)$, $\rho_{\text{ave,toluene}}=\rho_w\times(1-P)+\rho_{\text{toluene}}\times P$, where ρ_w, P, $\rho_{\text{ave,toluene}}$, and ρ_{toluene} are the density of the wall material between the pores, the porosity of the film, average mass density of the porous thin film saturated under toluene vapor and average mass density of toluene solvent, (0.865 g/cm^3). The porosity is defined as only those pores filled by the solvent.

From the measured critical angles, one can calculate the amount of toluene adsorbed and, hence, the porosity. The two unknowns, wall material density and porosity, are solved from these two equations providing a rigorous measurement of porosity and the average wall density. The wall density calculated by this method is an average of the wall material and any nonfilled pores such as closed pores and pores smaller than the toluene molecules. The wall density of the film prepared under a single frequency condition with N_2O oxidant shows the smallest value and around 80% and 50% of the wall density of the film deposited under dual frequency condition and O_2 atmosphere and the film density of thermally grown oxide, respectively.[9] The porosities of samples with varying process conditions ranged from 6% to 8% and are summarized in Table I. The SXR data of samples

TABLE I. Elemental composition and structural properties of α-SiCO:H films after varying process conditions. The relative standard uncertainties of the atomic composition, density, porosity, and film thickness are $\pm5\%$, 0.05 g/cm^3, 5%, and 50 Å, respectively.

Plasma condition	Dielectric constant	Atomic composition (Si:O:C:H:N, %)	Average density (g/cm^3)	Wall density (g/cm^3)	Porosity (%)	Thickness (Å)
N_2O, single	2.6	15: 10: 30: 40: 5	1.17	1.26	7	5130
N_2O, dual	2.7	15: 19: 20: 44: 2	1.23	1.31	6	4550
O_2, single	2.8	20: 36: 12: 32: 0	1.34	1.46	8	3020
O_2, dual	2.9	20: 36: 12: 32: 0	1.43	1.54	7	3230

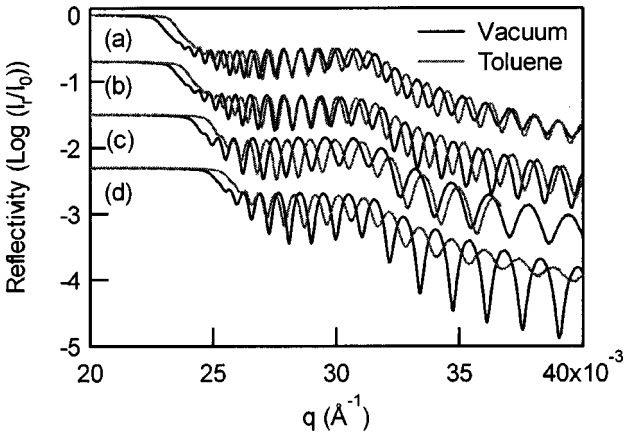

FIG. 3. SXR curves of α-SiCO:H films under a vacuum (black curves) and saturated in toluene (gray curves), (a) N_2O and single frequency, (b) N_2O and dual frequency, (c) O_2 and single frequency, and (d) O_2 and dual frequency.

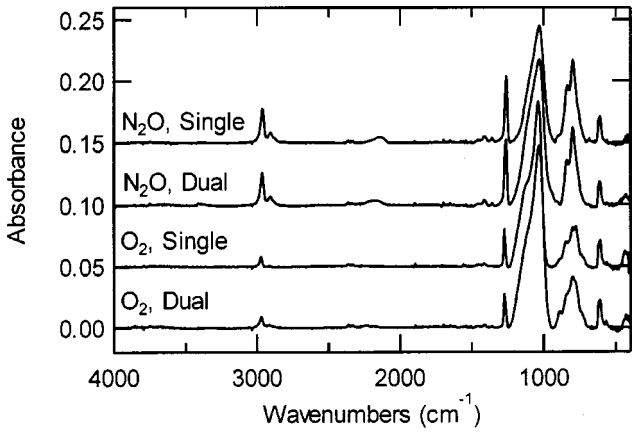

FIG. 4. FTIR spectra of α-SiCO:H films with different process conditions presented as the relative intensity of absorbance vs wave number. Curves are offset vertically for clarity.

saturated in toluene were fit. There were only slight differences in the density profiles from samples under a vacuum and saturated in toluene, primarily small increases in average density in the saturated toluene showing that that the size distribution of pores was uniform.

As shown from FTIR spectra in Fig. 4, the Si—O—Si stretching peak at $\approx$1060 cm^{-1} has a stronger shoulder at a higher wave number than those of the other samples. This shoulder is indicative of different types of chemical environments and has been reported as the stretching peak of the Si—O—Si bond in a caged structure.[12] Two additional absorption peaks due to the incorporated methylene group, $Si—CH_2—Si$ are clearly observed near 1370 cm^{-1} and 1430 cm^{-1}. The intensity of the methylene peak from the film deposited with N_2O is higher than that from the film deposited with O_2 as an oxidant. The deformation of the FTIR spectra Si—O—Si stretching peak $\approx$1100 cm^{-1} from the film prepared with the N_2O oxidant is consistent with a silica network partially modified by the replacement of the O atom with the CH_2 group.[13]

From these data, we propose the following description of the CVD deposition process. At the beginning of the film deposition, reactive intermediates with the methylene group are adsorbed onto the wafer surface and the methylene group is replaced by the oxygen atom without introducing internal strain.[13] Because oxygen radicals from the N_2O gas are less reactive than those from O_2 gas, some of methylene groups and methyl groups remain in the matrix without replacement of the oxygen atom. During film deposition under an O_2 atmosphere, the methyl moiety is removed from wall materials and the matrix becomes denser. At the same time, nanopores are generated during the removal of methyl moiety. Although the porosity of the α-SiCO:H low-k thin film prepared under a single frequency condition and the O_2 atmosphere has a slightly higher value, the differences in porosities among the samples are not significant. The average density is primarily determined by the density of wall material rather than the porosity. SANS measurements were performed to characterize the pore size of the films. The scattering intensity of the air sample arises from differences in the neutron scattering length of connecting wall material and the pores. These films had very weak scattering intensities indicating that the pore size and porosity are low. While the SANS measurements are not very sensitive to pore sizes smaller than 10 Å, this XRP method is useful for films with small pore sizes and low porosities because the diameter of a toluene molecule is approximately 6 Å, and SXR is very sensitive to changes in electron density.

We have applied XRP as a way of determining the existence of small pores and measured important structural and physical properties of trimethylsilane-based CVD silica films. The sensitivity of the x-ray reflectivity technique to density differences in films provides important insight into correlations between the structure of the porous thin films and processing parameters. The detailed quantitative measurements may be used by the semiconductor industry and materials scientists to optimize process conditions and design materials.

[1] M. McCoy, Chem. Eng. News **78**, 17 (2000).
[2] A. Grill and V. Patel, Appl. Phys. Lett. **79**, 803 (2001).
[3] T. L. Dull, W. E. Frieze, D. W. Gidley, J. N. Sun, and A. F. Yee, J. Phys. Chem. B **105**, 4657 (2001).
[4] M. R. Baklanov, K. P. Mogilnikov, V. G. Polovinkin, and F. N. Dultsev, J. Vac. Sci. Technol. B **18**, 1385 (2000).
[5] H. J. Lee, E. K. Lin, H. Wang, W. L. Wu, W. Chen, and E. S. Moyer, Chem. Mater. **14**, 1845 (2002).
[6] Certain commercial equipment and materials are identified in this letter in order to adequately specify the experimental procedure. In no case does such identification imply recommendation by the National Institute of Standards and Technology nor does it imply that the material or equipment identified is necessarily the best available for this purpose.
[7] M. J. Loboda, W. D. Gray, B. K. Hwang, J. A. Seifferly, and R. F. Schneider, Proceedings of the Advanced Metallization Conference, Montreal, Canada, 9–11 October 2001.
[8] H. J. Lee, E. K. Lin, W. L. Wu, B. M. Fanconi, H. C. Liou, J. K. Lan, Y. L. Cheng, Y. L. Wang, M. S. Feng, and C. G. Chao, J. Electrochem. Soc. **148**, F195 (2001).
[9] G. Ceriola, F. Iacona, F. L. Via, V. Raineri, E. Bontempi, and L. E. Depero, J. Electrochem. Soc. **148**, F221 (2001).
[10] L. G. Parratt, Phys. Rev. **95**, 359 (1954).
[11] The data throughout the manuscript and in Figs. 1–4 and Table I are presented along with the standard uncertainty ($\pm$) involved in the measurement based on one standard deviation.
[12] L. M. Han, J. S. Pan, S. M. Chen, N. Balasubramanian, J. Shi, L. S. Wong, and P. D. Foo, J. Electrochem. Soc. **148**, F148 (2001).
[13] S. Sugahara, T. Kadoya, K. Usami, T. Hattori, and M. Matsumura, J. Electrochem. Soc. **148**, F120 (2001).